Journal of Physics: Conference Series

PAPER • OPEN ACCESS

The dynamic recrystallization behavior in Al-Mg alloys

To cite this article: Yu Borisova *et al* 2019 *J. Phys.: Conf. Ser.* **1270** 012050

The dynamic recrystallization behavior in Al-Mg alloys

Yu Borisova, A Kalinenko, D Yuzbekova and A Mogucheva

Belgorod State University, Belgorod 308015, Russia

Corresponding author: borisova_yu@bsu.edu.ru

Abstract. The influence of phase composition on the behavior of dynamic recrystallization in alloys Al-3Mg (A1), Al-4.57Mg-0.35Mn-0.2Sc-0.09Zr (A2) and Al-5.4Mg-0.52Mn-0.1Zr (A3) (wt.%) during the equal-channel angular pressing (ECAP) was studied. The ECAP processing of alloy A1 resulted in a partially recrystallized microstructure with the mean size of coarse and fine grains of 20 and 1.4 µm, respectively In contrast, the formation of fully-recrystallized microstructure was observed in the alloys A2 and A3. The mean grain sizes in the alloys A2 and A3 were 1.1 and 1.5 µm, respectively. The hardness values in the alloys A2 and A3 after ECAP processing were increased by about 30% more than those in the alloy A1. This may be attributed to the presence of Al_6Mn and $Al_3(Sc,Zr)$ particles.

Keywords – Aluminum alloys, Dynamic recrystallization, Equal-channel angular pressing

1. Introduction

In recent decades, the refinement of the grain structure of aluminum alloys in order to obtain a fine-grained microstructure, i.e. microstructure with a grain size less than 1 micron, aroused a great attention. The great interest in fine-grained materials is primarily due to the possibility of improving their characteristics and achieving a new level of physical and mechanical properties [1-3]. Dynamic recrystallization (DRX) is an important mechanism controlling the formation of fine-grained microstructure for obtaining the required properties in various materials [4–7]. The most significant advantage of DRX is that the required microstructure can be formed directly during hot deformation [4,6,8].

The microstructures formed during DRX depend significantly on the temperature, strain and strain rate. In particular, the pressing technologies adhere to the strategy of applying large reductions, which lead to significant values of the strain. However, after reaching a certain strain, the final properties of the products are determined by the temperature and strain rate [9].

The formation of the fine-grained microstructure during hot deformation of aluminum alloys was fairly clarified [10]. This study dealt with the effect of deformation and heat treatment on the recrystallization and polygonization processes. However, little attention has been paid to the influence of the phase composition on the developing dynamic recrystallization in various aluminum alloys. The purpose of this work is to study the effect of phase composition on the DRX development in aluminum alloys.

2. Materials and method

IOP Conf. Series: Journal of Physics: Conf. Series **1270** (2019) 012050 doi:10.1088/1742-6596/1270/1/012050

In present work, the following aluminum alloys with different chemical composition were investigated. Alloy A1: Al-3Mg (wt.%); alloy A2: Al-4.57Mg-0.35Mn-0.2Sc-0.09Zr (wt.%); alloy A3: Al-5.4Mg-0.52Mn-0.1Zr (wt.%). Alloy A1 was produced by direct chill casting. The obtained ingots were homogenized at 500°C for 4 h, followed by slow cooling in the furnace. Then, billets with cross-section of 20 × 20 mm^2 and a length of 110 mm were subjected to a two-stage ECAP at a temperature of 300°C to a strain of ~ 8 and at a temperature of 200°C to a strain of ~ 4. Alloy A2 was obtained by continuous casting. The ingots of this alloy were subjected to homogenization annealing at 360–380°C for 12 h. For the formation of a fine-grained microstructure, ECAP was carried out at a temperature of 300°C to a strain of ~ 12. The initial microstructure of alloy A2 contained non-coherent Al_6Mn particles and coherent Al_3(Sc, Zr) particles. A3 alloy was obtained by continuous casting. The obtained ingots were subjected to homogenization annealing at 360°C for 6 h. The ECAP of the A3 alloy was carried out at 300°C to a strain of ~ 12. In this alloy, a fine-grained microstructure with non-coherent Al_6Mn particles was formed after ECAP processing.

The structural parameters were studied using the orientation imaging microscopy (OIM) with automated indexing of electron back scattering diffraction (EBSD) patterns using a Quanta 600 FEG scanning electron microscope (SEM). For the microstructure examination, the EBSD maps with a size of 100 × 100 μm^2 and a step of 0.2 µm were obtained. Due to the experimental error of the EBSD method, all low-angle boundaries with a misorientation of less than 2° were excluded from consideration using the TSL software. The misorientation of 15° was used as a criterion for distinguishing low- and high-angle boundaries (LAB and HAB, respectively).

3. Results and discussion

3.1. Initial microstructure

The initial microstructures of the studied alloys before ECAP represent a coarse-grained (CG) state. The initial microstructure of the alloy A1 consists of large grains with an average size of about 40 µm. No evidence of secondary phase particles in the alloy A1 in CG state is observed. The microstructure of alloy A2 consists of coarse elongated grains with a transverse size of ~ 20 µm and Al_3(Sc, Zr) particles with coherent interfaces and incoherent Al_6Mn particles distributed homogeneously throughout the matrix. The study of the microstructure of the alloy A3 in the CG state reveals the mean grain size of 22 µm. The uniform distribution of incoherent Al_6Mn particles is also observed inside the grains in this state. The dislocation densities in the studied alloys in CG state are approximately 10^{13} m^{-2}. Some parameters of the microstructures of studied alloys are presented in Table 1.

Table 1. Microstructure and mechanical properties of aluminum alloys.

Alloys	A1		A2		A3	
State	CG	FG	CG	FG	CG	FG
Grane size, µm	40	1.4 and 20	20	1.1	22	1.5
Fraction HAB's, %	84	48	35	78	93	62
Average Misorientation Angle, °	21	23	18	33	12	27
Microhardness, HV	55	95	97	129	94	128

3.2. Microstructure after ECAP

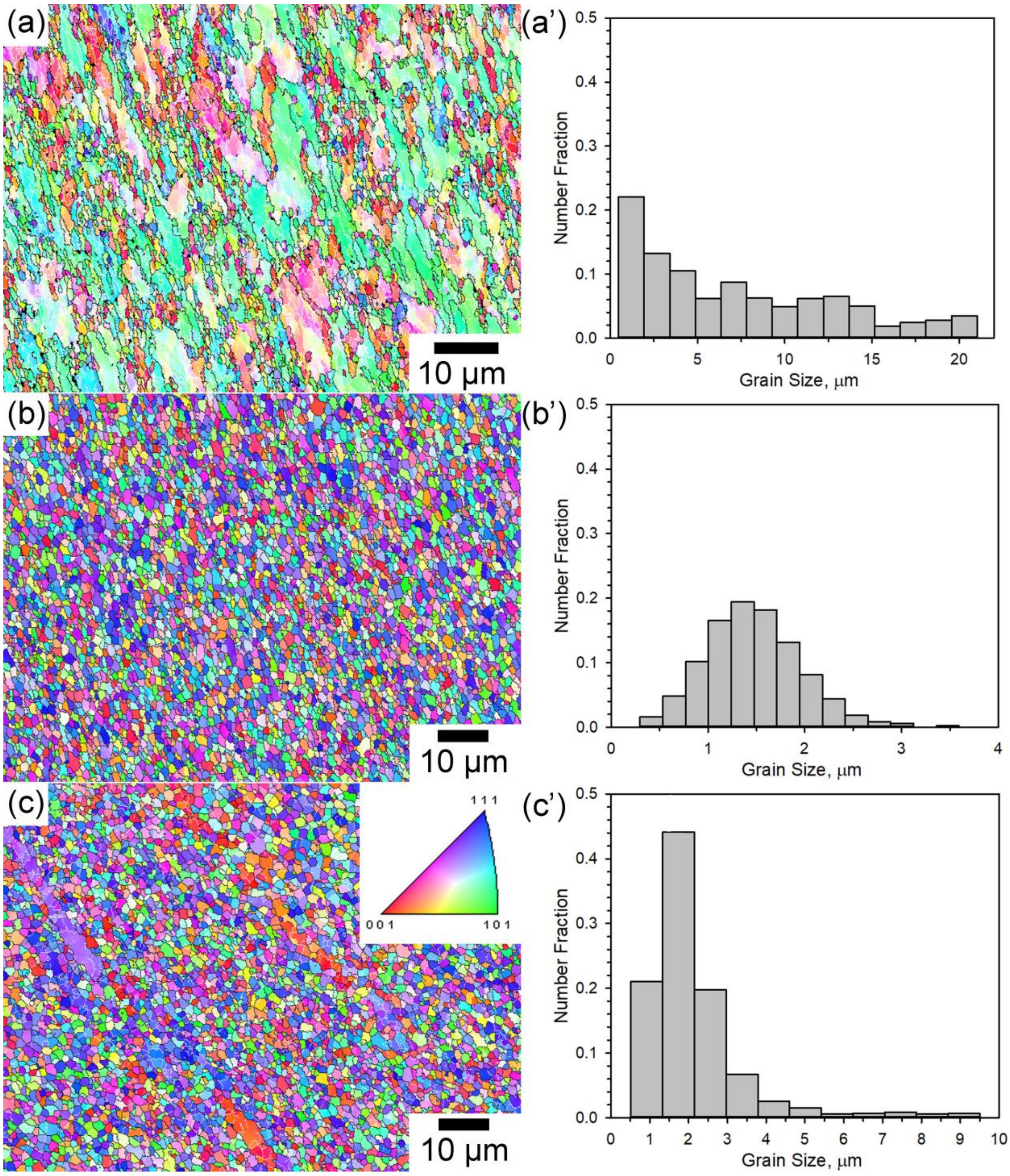

Figure 1. EBSD misorientation maps (a-c) and grain size distributions (a'-c') of the alloys A1 (a, a'), A2 (b,b') and A3 (c,c'). On the EBSD maps, the low-angle and high-angle boundaries are indicated by white and black lines, respectively.

A typical recrystallized microstructure, which develops during ECAP at 300°C, is shown in figure 1 and table 1. The bimodal grain size distribution is observed in alloy A1, where the partially-recrystallized microstructure consists in both the large and fine-grains (FG). It can be seen in figure 1a that the coarse remnants of original grains are surrounded by numerous fine recrystallized grains after 12 passes of ECAP. Thus, in the partially recrystallized microstructure shown in figure 1a, so-called microstructure of the necklace develops. The mean size of the coarse and fine grains in this state are 20 and 1.4 μm respectively. For all studied alloys, the fraction of recrystallized grains increases with an increase in the number of ECAP passes. The formation of new recrystallized grains occurs along the initial grain boundaries [11-13]. It is clearly seen in figures 1b and 1c that the homogeneous fine-grained microstructures are completely formed after 12 passes of ECAP in alloys A2 and A3. The average grain sizes in the alloys A2 and A3 are 1.1 and 1.5 μm respectively.

It should be noted that the grain sizes in the alloys A2 and A3 subjected to ECAP, are smaller than in A1, subjected to ECAP at the same temperature [14]. It is known [14] that the several alloying elements lead to substantial solid-solution hardening and slow down the recovery process. Such elements also lead to more pronounced grain refinement during severe plastic deformation. It is known that dissolved zirconium significantly slows down the diffusion processes in the aluminum matrix [15], preventing recovery and inhibiting the migration of grain boundaries. As a result, the size of recrystallized grains is reduced. Thus, in the alloys A2 and A3, the combined effect of pinning pressure from the Al_6Mn particles and dissolved zirconium results in much lower grain sizes as compared to that in the alloy A1 [14].

The fine-grained microstructures of the studied alloys are characterized by large fractions of LAB. In the alloy A1, the largest fraction of LAB and the higher value of the average misorientation angle θav as compared to other studied alloys are observed (figure 2). The average misorientation angles in the alloys A2 and A3 increase by 15° after ECAP processing. Note that a gradual increase in the average misorientation angle in these alloys is associated with a gradual increase in the fraction of the high-angle boundaries during deformation.

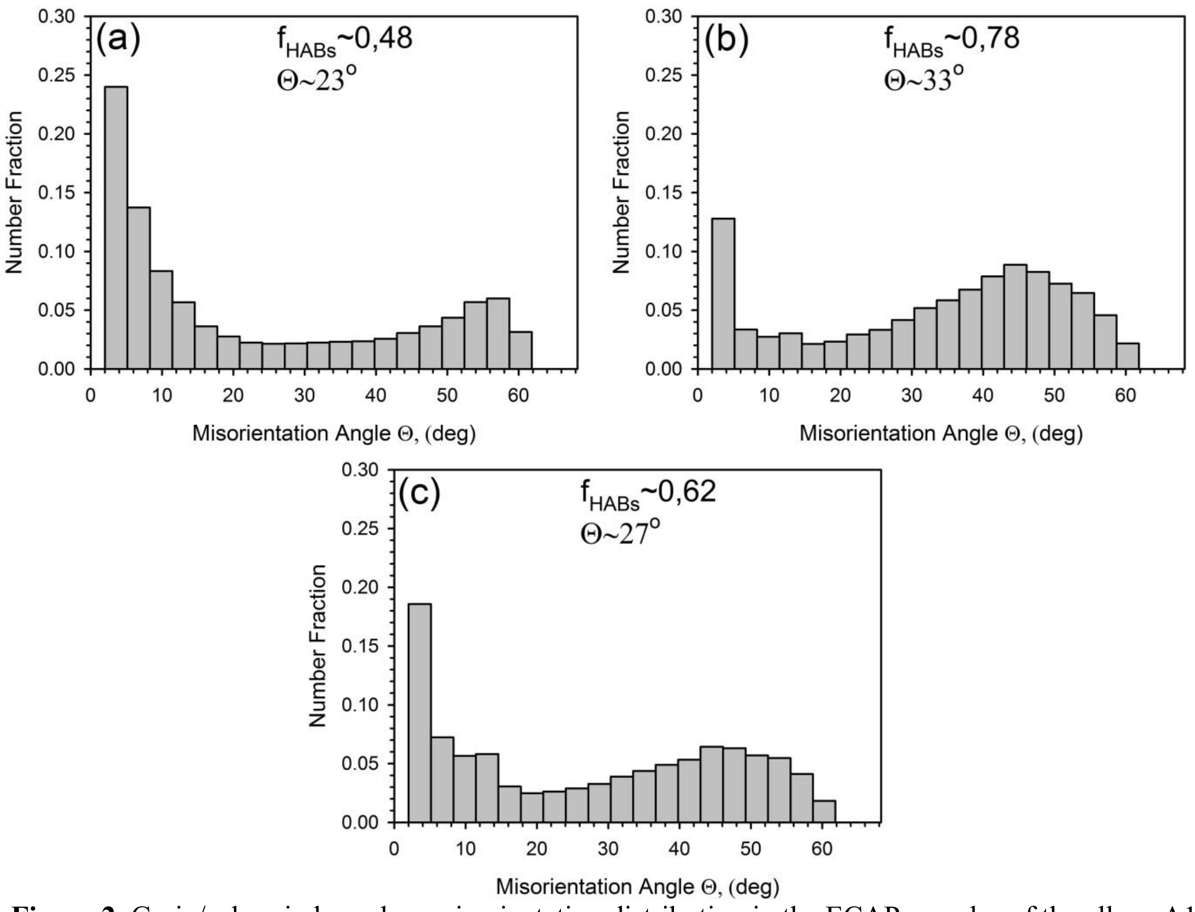

Figure 2. Grain/subgrain boundary misorientation distribution in the ECAP samples of the alloys A1 (a), A2 (b), and A3 (c).

IOP Conf. Series: Journal of Physics: Conf. Series **1270** (2019) 012050 doi:10.1088/1742-6596/1270/1/012050

An average lattice dislocation density was evaluated from the EBSD data from the lattice curvature using the kernel average misorientation option [16] via Frank's equation:

$$\Theta = 2\sin\frac{\Theta}{2} = \frac{Nb}{h} \tag{1}$$

where θ is the misorientation created by a wall consisting of N dislocations of height h, and b is the Burgers vector. In EBSD observations, distance h corresponds to the step size of the scanning. The dislocation density ρ is then given by the ratio of the dislocation number per surface area, Eq. (2):

$$\rho = \frac{N}{S} \tag{2}$$

where the surface area of the hexagon S (scanning geometry) is $S = \sqrt{3}h^2/2$. It follows that the dislocation density can be estimated from the following relationship:

$$\rho = \frac{2\Theta}{\sqrt{3}hb} \tag{3}$$

The values used for dislocation density calculations are given in table 2.

Table 2. Values of physical parameters in Eq. (3)

Alloys	h, μm	θ/h, m^{-1}	b, m	ρ, m^{-2}
A1	0.2	1.15×10^{5}	2.86×10^{-9}	2×10^{14}
A2	0.2	1.65×10^{5}	2.86×10^{-9}	1.5×10^{14}
A3	0.2	1.35×10^{5}	2.86×10^{-9}	1.4×10^{14}

For the alloy A1 the ECAP processing leads to 70% increase in hardness as compared to the CG state. The increase in hardness in alloys A2 and A3 is less pronounced. However, the hardness values in these alloys after ECAP is even higher than that in the A1 alloy, which may be due to the influence of Al_6Mn particles [17].

4. Summary and conclusions

In the present work, the influence of the phase composition on the DRX process in three aluminum alloys was investigated. The main results are as follows:

1. ECAP processing leads to the partially recrystallized microstructure in alloy A1. Such microstructure can be referred to as necklace microstructure. In the A2 and A3 alloys, fully recrystallized fine-grained microstructures are observed. The completion of DRX process in these alloys may be associated with the presence of $Al_3(Sc,Zr)$ and Al_6Mn particles.
2. The higher fraction of LABs and the smaller value of the average misorientation angle are observed in alloy A1 as compared to alloys A2 and A3. ECAP leads to an increase of the average misorientation angle by 15° in the A2 and A3 alloys.
3. The hardness of the alloys A2 and A3 is higher by approximately 30% than that in the A1 alloy. This may be due to the presence of incoherent Al_6Mn particles and coherent $Al_3(Sc,Zr)$ particles in the alloys A2 and A3.

Acknowledgement

The study was financially supported by the Russian Science Foundation, Belgorod State University project No. 17-72-20239. The main results were obtained by using the equipment of the Joint Research Center, «Technology and Materials», Belgorod State University.

References

[1] Markushev M, Vinogradov A 2006 *Severe Plastic Deformation: Towards Bulk Production of Nanostructured Materials* (Burnhanettin A. USA: Nova Science Publishers) P. 233–247.
[2] Dao V, Lu L, Azaro R et al. 2007 *Acta Materialia* vol 55 (Amsterdam: Elsevier) p 4041.
[3] Sitdikov O, Avtokratova E, Sakai T, Tsuzaki K 2013 *Metallurgical and Materials Transactions A* vol. 44 (Berlin, Germany: Springer) p 1087.
[4] Sakai T, Belyakov A, Kaibyshev R, Miura H, Jonas J.J 2014 Progress in Materials Science vol 60 (Amsterdam: Elsevier) p 130.
[5] Humphreys F, Hatherly M 2004 *Recrystallization and Related Annealing Phenomena* (Elsevier Science: New York, NY, USA).
[6] Huang K, Logé R 2016 Materials & Design vol 111 (Amsterdam: Elsevier) p 548.
[7] Zhang D, Yang X, Fang Z, Xiao Z, Yang Y, Sakai T 2016 *Materials Science and Engineering: A* vol. 675 (Amsterdam: Elsevier) p 128.
[8] Zhaoa P, Wanga Y, Niezgodaab S R 2018 International Journal of Plasticity vol 100 (Elsevier) p 52.
[9] Loginov Yu, Antonenko L 2010 *Zagotovitel'nyye proizvodstva v mashinostroyenii* [Preparation production in mechanical engineering] vol. 7 (Moscow: Innovative Engineering Press) p 14
[10] Trifonov V, Bobruk E 2004 *The Physics Of Metals And Metallography* vol 97 (Road Town: Pleiades Publishing, Ltd) p 188.
[11] Sakai T, Jonas J 1984 *Acta Metallurgica* vol 32 (Elsevier Science Publishing Company) p 189.
[12] Humphreys F, Hatherly M 2004 *Recrystallization and Related Annealing Phenomena* (Elsevier Science: New York, NY, USA).
[13] Dudova N, Belyakov A, Sakai T, Kaibyshev R 2010 *Acta Materialia* vol 58 (Amsterdam: Elsevier) p 3624.
[14] Sitdikov O, Sakai T, Avtokratova E, Kaibyshev R, Tsuzaki K, Watanabe Y 2008 *Acta Materialia* vol 56 (Amsterdam: Elsevier) p 821.
[15] Doherty R, Hughes D, Humphreys F. Jonas J, Jensen D, Kassner M, King W, T.R. McNelley, McQueen H, Rollett A 1997 *Materials Science and Engineering: A* vol. 238 (Amsterdam: Elsevier) p 219.
[16] Zhilyaeva A, Shakhova I, Morozova A, Belyakov A, Kaibyshev R 2016 *Materials Science and Engineering: A* vol. 654 (Amsterdam: Elsevier) p 131.
[17] Sato Y, Kokawa H, Enmoto M, Jogan S 1999 *Metallurgical and Materials Transactions A* vol. 30 (Berlin, Germany: Springer) p 2429.